Epitope-tagged P_0 Glycoprotein Causes Charcot-Marie-Tooth–like Neuropathy in Transgenic Mice

Stefano C. Previtali,* Angelo Quattrini,* Marina Fasolini,* Maria Carla Panzeri,‡ Antonello Villa,‡§ Marie T. Filbin,‖ Wenhui Li,‖ Shing-Yan Chiu,¶ Albee Messing,** Lawrence Wrabetz,* and M. Laura Feltri*

*Department of Neurology and Department of Biological and Technological Research (DIBIT) and ‡MIA-DIBIT, San Raffaele Scientific Institute, 20132 Milan, Italy; §University of Milano-Bicocca, Monza, Italy 20052; ‖Hunter College, New York, New York 10021; ¶Department of Physiology, School of Medicine, and **Waisman Center and Department of Pathobiological Sciences, School of Veterinary Medicine, University of Wisconsin, Madison, Wisconsin 53705

Abstract. In peripheral nerve myelin, the intraperiod line results from compaction of the extracellular space due to homophilic adhesion between extracellular domains (ECD) of the protein zero (P_0) glycoprotein. Point mutations in this region of P_0 cause human hereditary demyelinating neuropathies such as Charcot-Marie-Tooth. We describe transgenic mice expressing a full-length P_0 modified in the ECD with a myc epitope tag. The presence of the myc sequence caused a dysmyelinating peripheral neuropathy similar to two distinct subtypes of Charcot-Marie-Tooth, with hypomyelination, altered intraperiod lines, and tomacula (thickened myelin). The tagged protein was incorporated into myelin and was associated with the morphological abnormalities. In vivo and in vitro experiments showed that P_0myc retained partial adhesive function, and suggested that the transgene inhibits P_0-mediated adhesion in a dominant-negative fashion. These mice suggest new mechanisms underlying both the pathogenesis of P_0 ECD mutants and the normal interactions of P_0 in the myelin sheath.

Key words: Charcot-Marie-Tooth disease • myelin protein zero • tomacula • transgenic mice • Myc-tag

Introduction

Charcot-Marie-Tooth (CMT)[1] is the most frequent hereditary peripheral neuropathy in humans. The most common variant (CMT1A) is due primarily to the duplication of a large region of chromosome 17 that includes the gene for peripheral myelin protein-22 (*PMP-22*) (for review see Harding, 1995). In other cases, CMT1 and the more severe variants Déjérine-Sottas (DSS) syndrome and congenital hypomyelination (CH) are due to point mutations of the *PMP-22*, *GJ*β1, myelin protein zero (*MPZ*), or *EGR2* genes (reviewed in Nelis et al., 1999; Wrabetz et al., 2001). Thus, similar clinical entities are due to mutations of different genes involved in a common pathway that normally results in peripheral nerve myelination. However, different mutations in the same gene give rise to neuropathies of varying severity. For example, mutations in the *MPZ* gene may cause either CMT1B, DSS, or CH. These mutations are mostly localized in the extracellular domain (ECD) of the protein zero (P_0) glycoprotein, which is encoded by *MPZ* (for review see Nelis et al., 1999).

P_0, the most abundant protein in the peripheral nerve (Lemke et al., 1988), is a single pass transmembrane protein expressed in Schwann cells (SCs) that belongs to the immunoglobulin superfamily. P_0 acts as a homotypic adhesion molecule necessary for the formation of the intraperiod line (IPL) as myelin lamellae compact (D'Urso et al., 1990; Filbin et al., 1990; Schneider-Schaulies et al., 1990; Giese et al., 1992). Crystallographic analysis revealed that this adhesive function is probably mediated by the interaction of tetramers composed of ECD of P_0 molecules emanating from apposing lamellae (Shapiro et al., 1996). The P_0 null mouse supports such a role for P_0 and shows hypomyelination, widening and uncompaction of myelin lamellae, and slow nerve conduction velocity (Giese et al., 1992; Martini et al., 1995). The homozygous P_0 null mouse is considered a model of patients with DSS that are homozygous for predicted null mutations (e.g., Gly74 frameshift; Warner et al., 1996). The heterozygous P_0 null mouse presents a late onset, mild neuropathy and is a model for patients with CMT1B that are heterozygous for P_0 loss of function mutations (for review see Martini, 1997). However, it is likely that the majority of P_0 mutations act through gain of function, since, in most cases, they are dominantly inherited and cause a more se-

---

S.C. Previtali and A. Quattrini contributed equally to this work.

Address correspondence to Maria Laura Feltri, Department of Neurology and DIBIT 4A2, San Raffaele Scientific Institute, Via Olgettina 58, 20132 Milano, Italy. Tel.: 02-26-43-47-82. Fax: 02-26-43-47-67. E-mail: feltri.laura@hsr.it

[1]*Abbreviations used in this paper:* CMT, Charcot-Marie-Tooth; CH, congenital hypomyelination; DSS, Déjérine-Sottas syndrome; ECD, extracellular domain; GAPDH, glyceraldehyde-3-phosphate dehydrogenase; IPL, intraperiod line; MDL, major dense line; *Mpz*, myelin protein zero gene; nt, nucleotide; P, postnatal day; PMP-22, peripheral myelin protein 22; P_0, protein-zero; RT, reverse transcription; SC, Schwann cell; wt, wild-type.

vere phenotype than that of the heterozygous P_0 null mice (for review see Martini, 1997). Furthermore, the fact that some mutations may act through gain of function, and others through loss of function can explain, in part, the observation that mutations in the *MPZ* gene may cause either CMT1B, DSS, or CH.

Here, we describe the first transgenic mice that model CMT1B due to a gain of P_0 function. These mice were created by adding a randomly inserted P_0 transgene to two normal P_0 alleles to reveal only gain of function mechanisms. To follow intracellular trafficking of future P_0 mutants, normal P_0 was first tagged at the mature NH_2 terminus in the ECD. Crystallographic studies suggested that the NH_2 terminus of P_0 was not directly engaged in cis or trans interactions (Shapiro et al., 1996). P_0myc mice were created in parallel with mice in which overexpression of wild-type (wt) P_0 causes a developmental delay in myelination (Wrabetz et al., 2000). Surprisingly, P_0myc mice showed clinical and morphological abnormalities that were independent of P_0 overexpression. The morphological abnormalities resembled two subtypes of CMT1B patient, and the abnormalities worsened after outcrossing P_0myc into the P_0 null background. P_0myc was detected in abnormal myelin, and P_0myc was partially adhesive, as P_0myc expressed in P_0 null mice produced myelin with only a slight widening of IPLs, and in vitro, P_0myc aggregated transfected cells equally to wt P_0. These data suggest that P_0myc acts by a dominant-negative gain of function and have implications for normal P_0 interactions in myelin. P_0myc mice support the idea that the pathogenesis of some mutations in the ECD of P_0 includes gain of function.

Materials and Methods

Transgenic Mice, Genomic Analysis, Breeding, and Genetic Backgrounds

The transgene derives from mP_0TOT (Wrabetz et al., 2000) that contains the complete P_0 gene with 6 kb of promoter, all exons and introns, and the natural polyadenylation site (see Fig. 1). In $mP_0TOT(myc)$, an oligonucleotide encoding myc tag (5′-CCATTGAGCAAAAGCTCATTTCTGAA-GAGGACTTGAATG-3′) was inserted in frame into the MscI site in P_0 exon 2, corresponding to the NH_2 terminus of the mature P_0 protein (see Fig. 1) and recreated the signal peptide cleavage site. The myc oligonucleotide was first inserted into the plasmid $mP_05.7$ (Wrabetz et al., 2000) to create $mP_05.7myc$. A 7-kb EcoRI fragment was excised from the plasmid mP_0E (Wrabetz et al., 2000) and ligated into EcoRI-digested $mP_05.7myc$ to generate the plasmid $mP_0TOT(myc)$. $mP_0TOT(myc)$ contains a polymorphic BglII site in exon 3 (amino acid sequence is conserved) that is not present in the endogenous FVB/N P_0 alleles. For oocyte injection, the transgene was excised from the vector using XhoI and NotI. Transgenic mice were generated by standard techniques (Brinster et al., 1985) using fertilized eggs obtained from the mating of FVB/N mice (Taconic). Transgenic lines were maintained by backcrosses to FVB/N mice (Taconic or Charles River). Founders that transmitted the transgene to progeny were identified by Southern blot and PCR analysis of genomic DNA, which were prepared from tail samples, as described previously (Feltri et al., 1999; Wrabetz et al., 2000). The genetic designations of the three lines that have been maintained from this study are: line 88.1,TgN(Mpzmyc)19Mes; line 88.2,TgN(Mpzmyc)20Mes; and line 88.4, TgN(Mpzmyc)21Mes.

P_0 null mice ($P_0^{+/-}$ and $P_0^{-/-}$) were identified by Southern blot and PCR analysis of tail genomic DNA, as described (Wrabetz et al., 2000). P_0 null mice were backcrossed into the FVB/N background. The N5 generation $P_0^{+/-}$ was crossed with transgene 88 (P_0myc) FVB to obtain N6 $P_0^{+/-}$/P_0myc. Subsequent crosses of N6 $P_0^{+/-}$/P_0myc with N6 $P_0^{+/-}$ gave rise to the F1N6 generation that was analyzed for rescue, as a consequence of reduced P_0 dosage. $P_0^{+/-}$/P_0myc and $P_0^{-/-}$/P_0myc mice were identified by Southern blot. The presence of a 2.1-kb band identified the null allele (Wrabetz et al.,

2000), whereas the myc transgene was identified after densitometry and PCR analysis by the presence of an intense 1.0-kb band. In $P_0^{-/-}myc$, the 6.8-kb band from the wt *Mpz* allele was absent (data not shown).

All the experiments involving animals were described in protocols approved by the San Raffaele Scientific Institute Institutional Animal Care and Use Committee. Animals that showed signs of distress due to neuropathy were killed.

Electrophysiologic Analysis

The compound muscle action potential and nerve conduction velocity of transgenic mice and control littermates at postnatal day (P) 42 were measured as described (Wrabetz et al., 2000).

Morphology

Transgenic mice and age-matched controls were killed at the ages indicated, and semithin and ultrathin morphological analysis were conducted as previously described (Quattrini et al., 1996). To quantitate the amount of abnormal myelin periodicity after crossing into the P_0 null background, at least 100 myelinated fibers for each genotype were counted at a magnification of 7,000× in 10 random, independent fields; abnormally compacted fibers were expressed as the percent of total fibers.

Immunohistochemistry and Immunoelectron Microscopy

For cryosections, sciatic nerve segments were fixed for 1 h in 4% paraformaldehyde in 0.1 M PBS, cryoprotected in 20% sucrose, embedded in OCT (Miles), and snap frozen in liquid nitrogen. Indirect immunofluorescence was performed on transverse and longitudinal cryosections. Cryosections (8-μm thick) were fixed in cold acetone for 2 min, rinsed twice in PBS, and blocked with 10% normal goat serum (Dako). Double staining was performed with a rabbit pAb recognizing P_0, (a gift from Dr. D. Colman, Mount Sinai School of Medicine, New York, NY) (Colman et al., 1982), and an mAb recognizing myc (American Type Culture Collection; clone 1-9E10.2), diluted 1:200 and 1:20, respectively. Sections were then treated with FITC- or TRITC-conjugated secondary antibodies (Southern Biotechnology Associates, Inc.), and examined with confocal microscopy (MRC 1024; Bio-Rad Laboratories).

For electron microscopic immunocytochemistry, segments of sciatic nerves were fixed with 4% paraformaldehyde and 0.25% glutaraldehyde in 125 mM PBS, pH 7.4, for 2 h. The samples were infiltrated with polyvinylpyrrolidone and frozen in a 3:1 (vol/vol) mixture of propane and isopentane cooled with liquid nitrogen. Ultrathin cryosections (50–100-nm thick) were cut using an Ultracut ultramicrotome, which was equipped with a Reichert FC4 cryosectioning apparatus and processed as described previously (Villa et al., 1993). In brief, the cryosections were collected over nickel grids and covered with 2% gelatin. After treatment with 125 mM PBS supplemented with 0.1 M glycine, they were double-immunostained with primary antibodies anti-P_0 and anti-myc diluted in PBS-glycine buffer. Gold-labeled secondary antibodies (British Biocell International) diluted 1:80 in PBS-glycine buffer recognized P_0 (small particles, 5 nm) and myc (large particles, 15 nm). Cryosections were then examined by EM.

Teased Fiber Preparation

Glutaraldehyde-fixed sciatic nerves from 6-mo-old P_0myc transgenic mice were osmicated and placed in glycerol. Single fibers were separated with fine forceps, placed on slides, and analyzed with a light microscope (Olympus).

Semiquantitative Reverse Transcribed-PCR

Total RNA isolation and reverse transcription (RT)-PCR were performed, as described previously (Wrabetz et al., 2000), on sciatic nerves from animals from P28. The RT-PCR assay was performed as a modification of the method by Fiering et al. (1995). The polymorphic BglII site spans the intron 2/exon 3 boundary, but in the cDNA product its four nucleotide (nt) core, a DpnII site, is still present. The validity of the method for semiquantitative assessments was verified using known amounts of templates, containing or not containing DpnII (Wrabetz et al., 2000). In the rescue experiments, RT-PCR was used to determine total levels of P_0 mRNA in P28 sciatic nerves, as previously described (Feltri et al., 1999). In brief, equal volumes of RT products were amplified using glyceraldehyde-3-phosphate dehydrogenase (GAPDH) specific primers (5′-GTATGACTCTACCCACGG-3′ and 5′-GTTCAGCTCTGG-GATGAC-3′) in the presence of $α^{32}$P-dCTP. Aliquots from the amplification
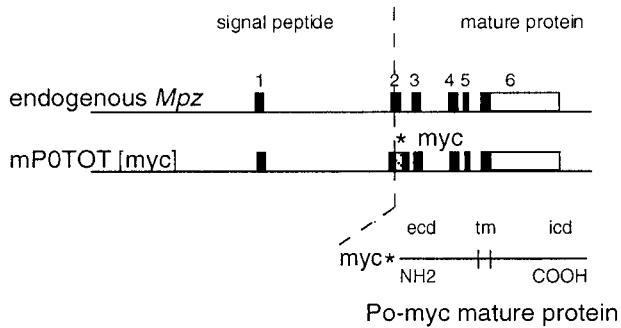
Figure 1. Design of P$_0$myc transgene. A schematic representation of the endogenous *Mpz* gene, the mP$_0$TOT(myc) transgene, and the mature P$_0$myc protein are shown. ecd, ectodomain; tm, transmembrane domain; icd, intracellular domain. Coding portions of exons are in black; the myc tag is hatched and marked by an asterisk.

were withdrawn at 22, 24, and 26 cycles, resolved on an acrylamide gel, and visualized by autoradiography. The intensity of the bands was quantified by densitometry (Molecular Dynamics) to verify that amplification was logarithmic and to determine the relative amount of starting cDNA from each sample. Equal amounts of reverse transcribed product, as determined by the GAPDH signal, were amplified using primers specific for P$_0$ (5′-GTCCAG-TGAATGGGTCTCAG-3′ and 5′-GCTCCCAACACCACCCCATA-3′). The intensity of the bands was quantified by densitometry, and the ratio between P$_0$ and GAPDH was determined.

Western Blot Analysis

Western blot analysis was performed, as described previously (Wrabetz et al., 2000), on sciatic nerves from P28 transgenic and nontransgenic littermates. To verify equal loading of proteins, membranes were stained with amido black. The primary antibodies used were: anti-myc (clone 1-9E10.2 ATCC), anti-P$_0$7 (a gift from Dr. J. Archelos, Karl-Franzens-Universitat, Graz, Austria) (Archelos et al., 1993). Peroxidase-conjugated second antibodies (Sigma-Aldrich) were visualized using the enhanced chemiluminescence method (NEN Life Science Products).

Aggregation Assay

To construct the pSJLrP$_0$myc plasmid, a MscI/BstE II fragment from plasmid mP$_0$5.7 myc was first cloned into rP$_0$pBSK+ (Filbin and Tennekoon, 1990). The P$_0$myc cDNA was then cloned into the XhoI site of pSJL (Filbin and Tennekoon, 1990) to create pSJLP$_0$myc. The hybrid cDNA used in transfection encodes a P$_0$myc with one conservative amino acid change relative to rat (val9ile; residue nine is ile in the mouse and val in rat and human); no mutations have been described at human P$_0$ val9. CHO cell transfection, expression, and adhesion essays were described previously (Filbin et al., 1990; Filbin and Tennekoon, 1993). In brief, a single cell suspension of P$_0$, P$_0$myc, or control cells was allowed to aggregate during rocking at 5 rpm at 37°C. Aggregate formation in samples withdrawn at various times was assessed by microscopic examination and by counting total particle number in a Coulter counter. Reduced total particle number is an indication of aggregate formation. The mixed adhesion assay was carried out as described previously (Wong and Filbin, 1996).

Image Analysis

Micrographs of morphological samples and radiographic films were digitalized using an AGFA Arcus 2 scanner and figures were prepared using Adobe® Photoshop 5.0.

Results

Transgenic Mice Expressing P$_0$myc Develop a Dysmyelinating Peripheral Neuropathy

The entire *Mpz* was reconstructed to contain 6 kb of the P$_0$ 5′ flanking sequence, all exons, the natural polyadenyla-

Lines and clinical phenotypes

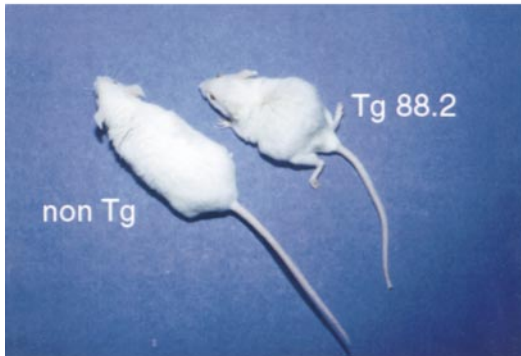| line	tremor	atrophy	ncv
Tg88.1	++	++	2±0.1
Tg88.2	+++	+++	n.d.
Tg88.4	+	-	15±2.7
Tg88.4/Po+/-	n.d.	n.d.	14±2.6
Tg88.1/ Po+/-	n.d.	n.d.	3±1.0
non Tg-	-	-	38±6.8

Figure 2. Lines, clinical phenotype, and nerve conduction velocities (ncv) are listed in the table, ncv are in m/s expressed as mean ± SEM (n = 2–4). In the photograph below, a P$_0$myc (Tg 88.2) animal at P160 manifests atrophy in axial and hindlimb muscles compared with a normal age-matched control (non Tg). −, absent; +, mild; ++, medium; and +++, severe.

tion signal and 400 flanking nts (mP$_0$TOT vector; Wrabetz et al., 2000). A derivative of mP$_0$TOT (mP$_0$TOTAn*lac*Z) was regulated in parallel with P$_0$ during postnatal development and after Wallerian degeneration (Feltri et al., 1999). Moreover, mP$_0$TOT was able to produce structurally and functionally normal myelin when expressed in the P$_0$$^{-/-}$ background (Wrabetz et al., 2000). To locate P$_0$ intracellularly, sequence encoding a myc tag was inserted into exon 2 (mP$_0$TOTmyc), downstream of the sequence coding for the signal peptide, to precede the NH$_2$ terminus in the extracellular portion of the mature protein (Fig. 1).

We produced four founder P$_0$myc mice, three of which (88.1, 88.2, and 88.4) transmitted the transgene to offspring. Mice from all lines displayed tremors and variable signs of muscle weakness, such as clenching of the paws, dragging of hind limbs, and floppy tail (Fig. 2). One line (88.2) manifested self-mutilation, presumably deriving from sensory symptoms. In two of the three lines (88.1 and 88.2), a marked muscular atrophy was evident (Fig. 2). All symptoms were most severe in line 88.2, intermediate in line 88.1, and least severe in line 88.4, corresponding to copy number and expression of the transgene, as estimated by Southern blot and RT-PCR analysis (see below and data not shown).

Since these symptoms are characteristic of a peripheral neuropathy, we measured nerve conduction velocity, which was significantly decreased in both lines tested (Fig. 2). These data indicate that the mice suffer from a dysmyelinating peripheral neuropathy.
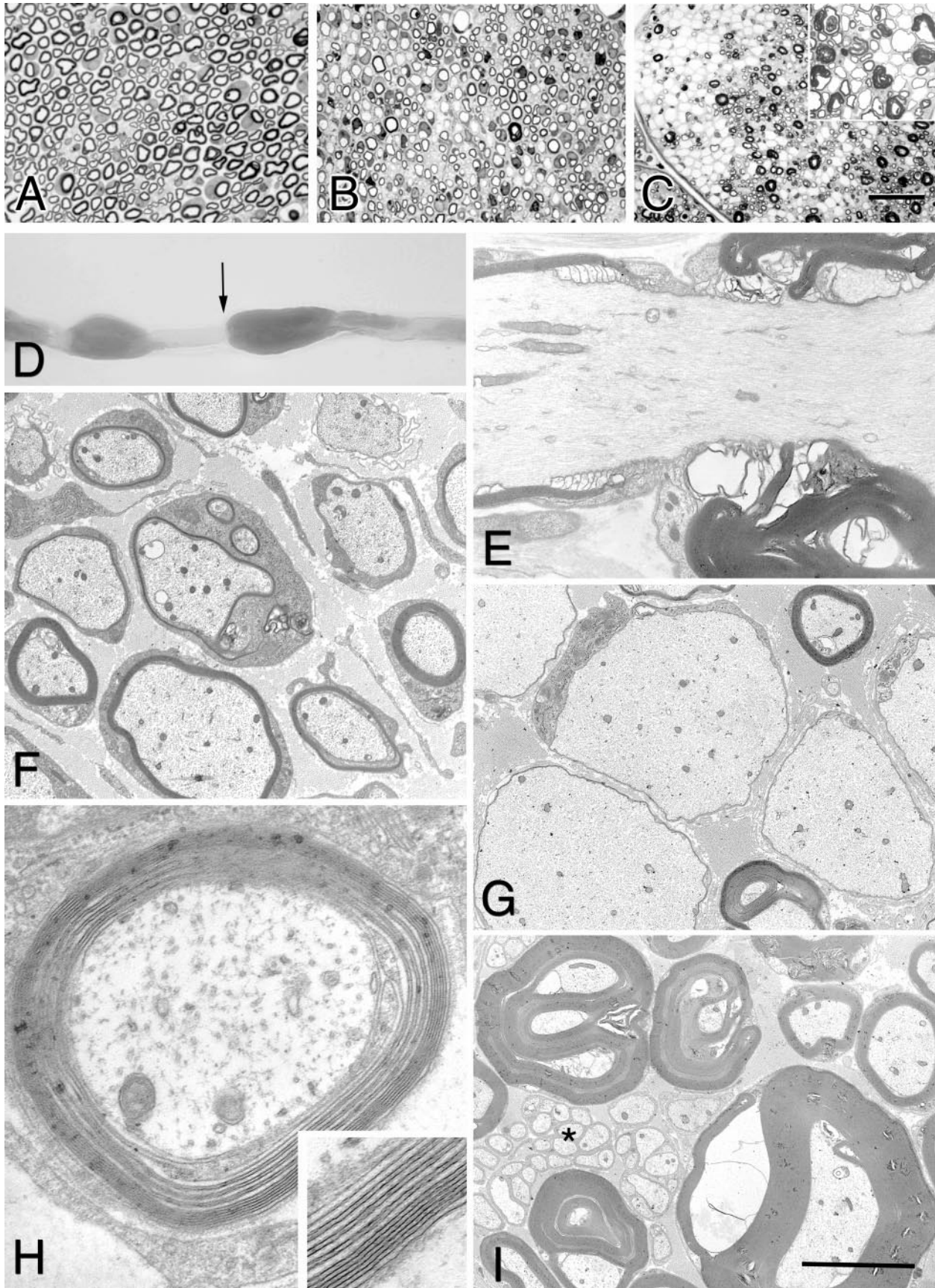
Figure 3. P_0myc nerves contain abnormal myelin compaction and tomacula. (A–C) Semithin section, (D) teased fiber, and (E–I) ultrastructural analysis of (A) wt, (B–G) P_0myc/Tg 88.1, and (H and I) P_0myc/Tg 88.2 sciatic nerves showing dysmyelination, tomacula, and widening of myelin lamellae. Transverse semithin sections stained with toluidine blue at (A and B) P28 showed diffuse hypomyelination and few abnormally outfolded myelin sheaths in P_0myc mice (tomacula-like). (C) At 7 mo, hypomyelination was still severe and the number of myelin out-
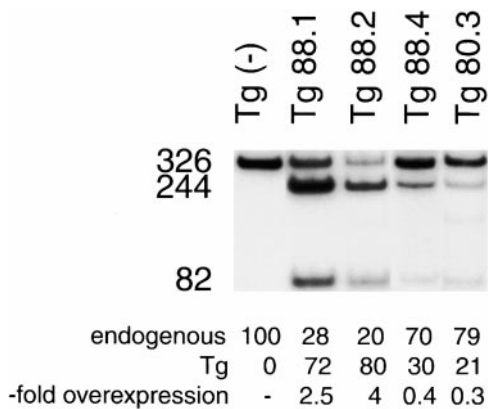
Figure 4. mP$_0$TOT(myc) transgene expression in sciatic nerve. Semiquantitative RT-PCR analysis from P28 sciatic nerves for endogenous *Mpz* and transgenic mRNA. Total RNA was reverse transcribed and the product amplified by PCR, using a primer pair that recognized identically both endogenous nontransgenic (Tg−) and transgenic (Tg88 and Tg80) P$_0$ cDNA. Due to a polymorphism present only in transgenic P$_0$, it is possible to distinguish bands of endogenous P$_0$ cDNA (326 nt) from transgenic P$_0$ cDNA (244 and 82 nt) after DpnII digestion. The relative proportion of transgenic and endogenous mRNA is shown, and the "-fold overexpression" is the quotient of the transgenic divided by the endogenous signal. This experiment shows that the transgenic mRNA is expressed in all lines. Note that the P$_0$myc/Tg88.4 ratio is similar to P$_0$wt-overexpressing/Tg80.3 line, which expresses below the threshold at which dysmyelination appears.

P$_0$myc Mice Resemble Subtypes of CMT1B

Morphological analysis of transgenic sciatic nerves at P28 showed hypomyelination, with thin or absent myelin sheaths on many large caliber axons, both at the light- and electron-microscopic levels (Fig. 3, B and F). Occasional fibers showed thick and redundant myelin, possibly representing myelin outfolding or tomacula. Ultrastructural analysis revealed that the myelin lamellae were widely spaced, in particular, the inner lamellae closer to the axon (Fig. 3 H). High magnification of the poorly compacted areas revealed absence of the IPL (inset). Occasionally, the major dense line (MDL) was also uncompacted. Similar packing abnormalities, especially at the innermost part of the myelin sheaths, have been described in several CMT1B patients carrying missense mutations in the ECD of P$_0$ (Gabreels-Festen et al., 1996; Kirschner et al., 1996b; Ohnishi et al., 1999). At seven months, the hypomyelination was more pronounced, with most of the large caliber axons showing very thin or absent myelin (Fig. 3 C). Several axons were enlarged and completely devoid of myelin (Fig. 3, C and G), whereas unmyelinated fibers appeared normal. In parallel, tomacula were more frequent (Fig. 3 C, inset). In teased fiber analysis or EM, the tomacula appeared to originate from the paranodal region (Fig. 3, D and E) and contained poorly compacted myelin (Fig. 3 I). Axonal caliber was pre-

served throughout the tomacula (Fig. 3 E). Similar tomacula were reported in a different group of CMT1B patients with mutations in the ECD of P$_0$ (Thomas et al., 1994; Gabreels-Festen et al., 1996; Tachi et al., 1997; Nagakawa et al., 1999; Planté-Bordeneuve et al., 1999; Sindou et al., 1999). Hypomyelination, tomacula, and uncompaction of the myelin sheath were readily observed in all three P$_0$myc lines. Occasionally, demyelinating figures, short internodes suggesting remyelination, and signs of axonal degeneration were observed in older mice (data not shown). In contrast, we never observed the presence of onion bulbs at any age in the P$_0$myc mice. Thus, it appears that the myc tag at the NH$_2$ terminus of the mature P$_0$ protein mimics some of the effects of P$_0$ mutations in the ECD.

Since P$_0$myc mice potentially overexpress P$_0$, we compared the morphology of mice expressing P$_0$myc (Tg 88) to mice overexpressing P$_0$wt (Tg 80; Wrabetz et al., 2000). Whereas widening of myelin lamellae and tomacula were present in all three P$_0$myc lines, we never observed them in any P$_0$wt insertion (eight independent insertions were examined for tomacula; of these, four were also examined for widened lamellae). Therefore, the morphological findings of P$_0$myc mice were distinct from those of P$_0$wt overexpressor mice.

The Phenotype of P$_0$myc Mice Is Independent of P$_0$ Overexpression

To determine the levels of mP$_0$TOT(myc) mRNA expression, we used RT-PCR analysis and exploited a DpnII polymorphism present in the transgenes, but not in endogenous *Mpz*. P$_0$ primers flanking the polymorphism amplify a 326-nt band from reverse transcribed sciatic nerve mRNA. After DpnII digestion, the 326-nt band corresponding to the endogenous P$_0$ remains uncut, whereas the transgenic P$_0$ cDNA is cleaved into two bands of 244 and 82 nt (Fig. 4).

We have previously shown that at ~0.5-fold overexpression of P$_0$ above normal levels in transgenic mice, a dose-dependent dysmyelination appears (hypomyelination and SC developmental delay) (Wrabetz et al., 2000). To confirm that the observed phenotype in P$_0$myc mice was not due to P$_0$ overexpression, we compared P$_0$ expression levels in P$_0$myc and P$_0$wt lines. We chose the P$_0$ line (80.3) that is just at the threshold of 0.5-fold P$_0$ overexpression necessary to cause dysmyelination. After DpnII digestion, the two bands of 244 and 82 nt, corresponding to the transgenic mRNA, were seen in all the P$_0$myc (88) and P$_0$wt (80.3) lines, but not in nontransgenic mice (Fig. 4). The 326-nt band corresponding to endogenous P$_0$ mRNA is seen in all samples. Densitometry revealed that P$_0$myc lines 88.1, 88.2, and 88.4 expressed P$_0$myc at 2.5-, 4-, and 0.4-fold above the level of endogenous *Mpz*, whereas the P$_0$wt line (80.3) expressed 0.3-fold (0.3–0.5-fold in other experiments, data not shown) of endogenous *Mpz*. Therefore, line 88.4 expresses at levels just at the threshold necessary to reveal an overexpression phenotype, yet it has the more severe phenotype similar to the other P$_0$myc

folding/tomacula rose (inset). Some axons appear enlarged and devoid of myelin (see also G). Teased fiber and electromicroscopic analysis of longitudinal sections at (D) 12- and (E) 7-mo-old in P$_0$myc showed that tomacula often originate at the paranodal region (arrow), and that the axon caliber is preserved underneath the tomacula. EM showed axons with absent or thin myelin sheaths at (F) P28 and demonstrated (H and inset) widely spaced myelin lamellae in many fibers. In 7-mo-old animals, hypomyelination, (G) enlarged amyelinated axons, and (G and I) myelin outfolding/tomacula containing poorly compacted myelin were prominent, whereas (I, asterisk) unmyelinated fibers appeared normal. Bar (in C): (A–C) 65 μm; (inset) 40 μm. Bar (in I): (D) 25 μm; (E) 3.5 μm; (F) 3 μm; (G) 5 μm; (H) 1 μm; (inset) 0.6 μm; (I) 6 μm.
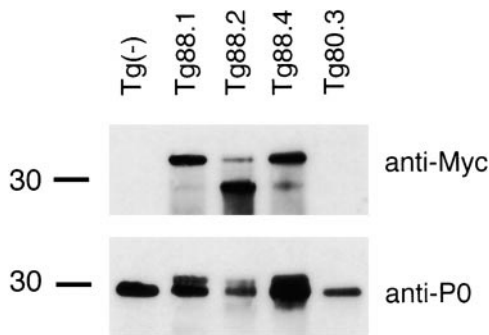
Figure 5. P_0myc protein expression in sciatic nerve. Western blot analysis performed on sciatic nerve lysates from P_0myc/Tg 88, P_0wt/Tg 80.3, and nontransgenic/Tg($-$) mice at P28. Anti-myc antibody recognized P_0myc only in P_0myc/Tg 88 nerve lysates (top), whereas anti-P_0 antibody recognized both P_0myc and P_0wt (bottom). The amount of P_0 reflects the effect of transgene over-expression (88.2 > 88.1 > 88.4) counteracted by the loss of P_0 due to dysmyelination (88.2 > 88.1 > 88.4). A relative molecular weight of 30 kD is indicated.

lines. A further reduction of transgene dosage, achieved by outcrossing the P_0myc/88.4 line with P_0 null mice (to obtain P_0myc/$P_0^{+/-}$ and P_0myc/$P_0^{-/-}$ mice) improved the hypomyelination, but not the widening of myelin lamellae and tomacula (see Fig. 7, and below). These data, taken together with the presence of morphological signs distinct from P_0-overexpressing mice, confirm that the phenotype of P_0myc mice is not due to overexpression of P_0.

P_0myc Protein Is Expressed in Transgenic Mouse Nerves

To evaluate if the transgenic protein was expressed in P_0myc mice, we performed Western blot analysis on sciatic nerve homogenates. Anti-myc antibody detected a band of ~33 kD, the appropriate size for P_0 plus myc, in all of the P_0myc lines, but not in nontransgenic littermates or in P_0wt mice (Fig. 5). In the P_0myc/88.2 line, the total levels of P_0 were reduced in association with the loss of bulk myelin, as previously found in P_0wt mice (Wrabetz et al., 2000). Endogenous P_0 was detected in all lanes using an anti-P_0 mAb; a larger band, corresponding to P_0myc, was again detected only in the P_0myc/88 lines. The smaller band seen with anti-myc, and sometimes with the anti-P_0 antibody, is probably a degradation product (Wrabetz et al., 2000). Amido black staining showed that comparable amounts of protein homogenates were loaded in each lane (data not shown). These data demonstrate that the transgenic protein was expressed in sciatic nerves of all lines.

P_0myc Protein Is Incorporated in the Myelin Sheath and Present in Widened Lamellae and Tomacula

Since P_0myc mice contain two normal *Mpz* alleles in addition to the transgene, and mP_0TOT(myc) is expressed at the level of mRNA and protein in transgenic sciatic nerves, P_0myc should exert its negative effect by a gain of function rather than a loss of function mechanism. If this is true, the myc-tagged P_0 should not only be expressed, but should also be incorporated in the myelin sheath, and possibly present in the pathological fibers. To test this, we first stained transgenic sciatic nerves by immunohistochemistry using P_0 pAb and myc mAb. By double immunofluorescence and confocal micros-
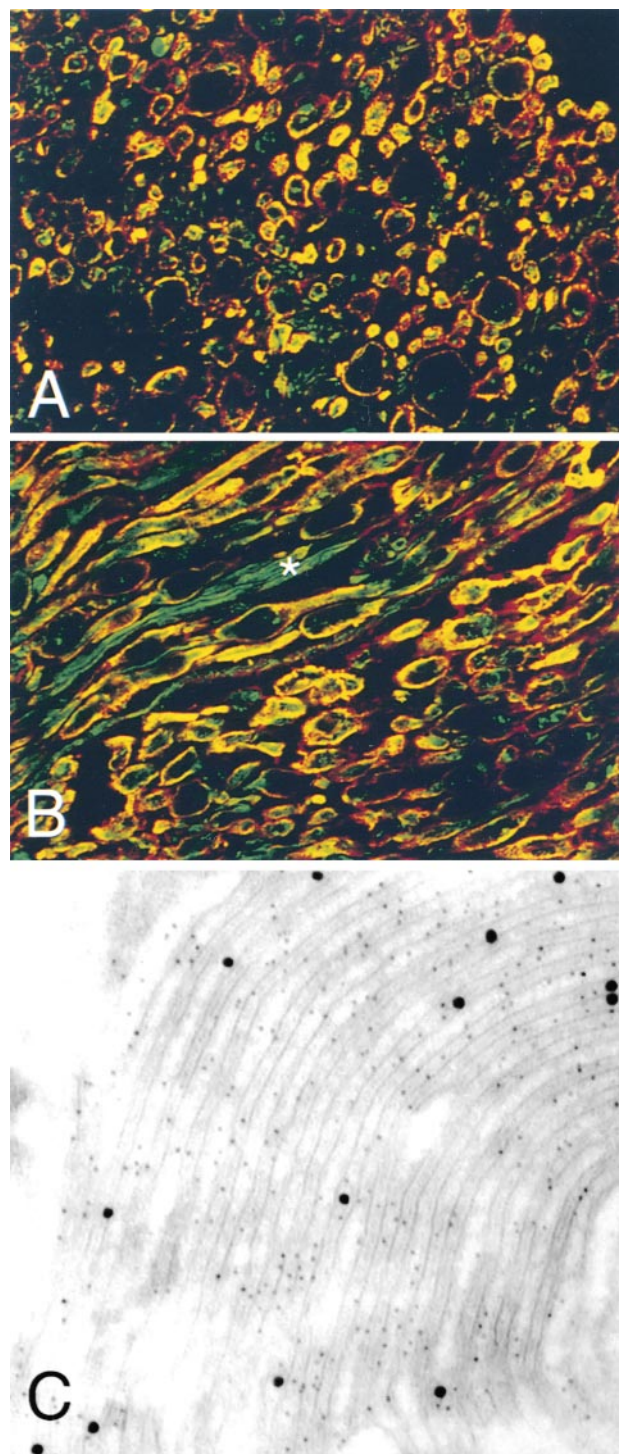

Figure 6. P_0myc is correctly inserted into myelin sheaths, in parallel with P_0wt. (A and B) Merged confocal images and (C) immunoelectron microscopy of P28 P_0myc/Tg 88.4 sciatic nerves cut (A and C) transversely or (B) longitudinally, and double stained with anti-myc (TITC or large gold particles) and anti-P_0 (FITC or small gold particles) antibodies. (A and B) Almost complete colocalization of the two signals was observed after merge (in yellow). Rare fibers did not stain for myc (e.g., green signal, asterisk). (C) Immunoelectron microscopy showed that P_0myc was present in areas containing widened myelin lamellae.

copy, we observed both P_0 (green fluorescence) and myc (red fluorescence) in compact myelin, and the signals often colocalized (Fig. 6 A). Longitudinal sections showed that myc was
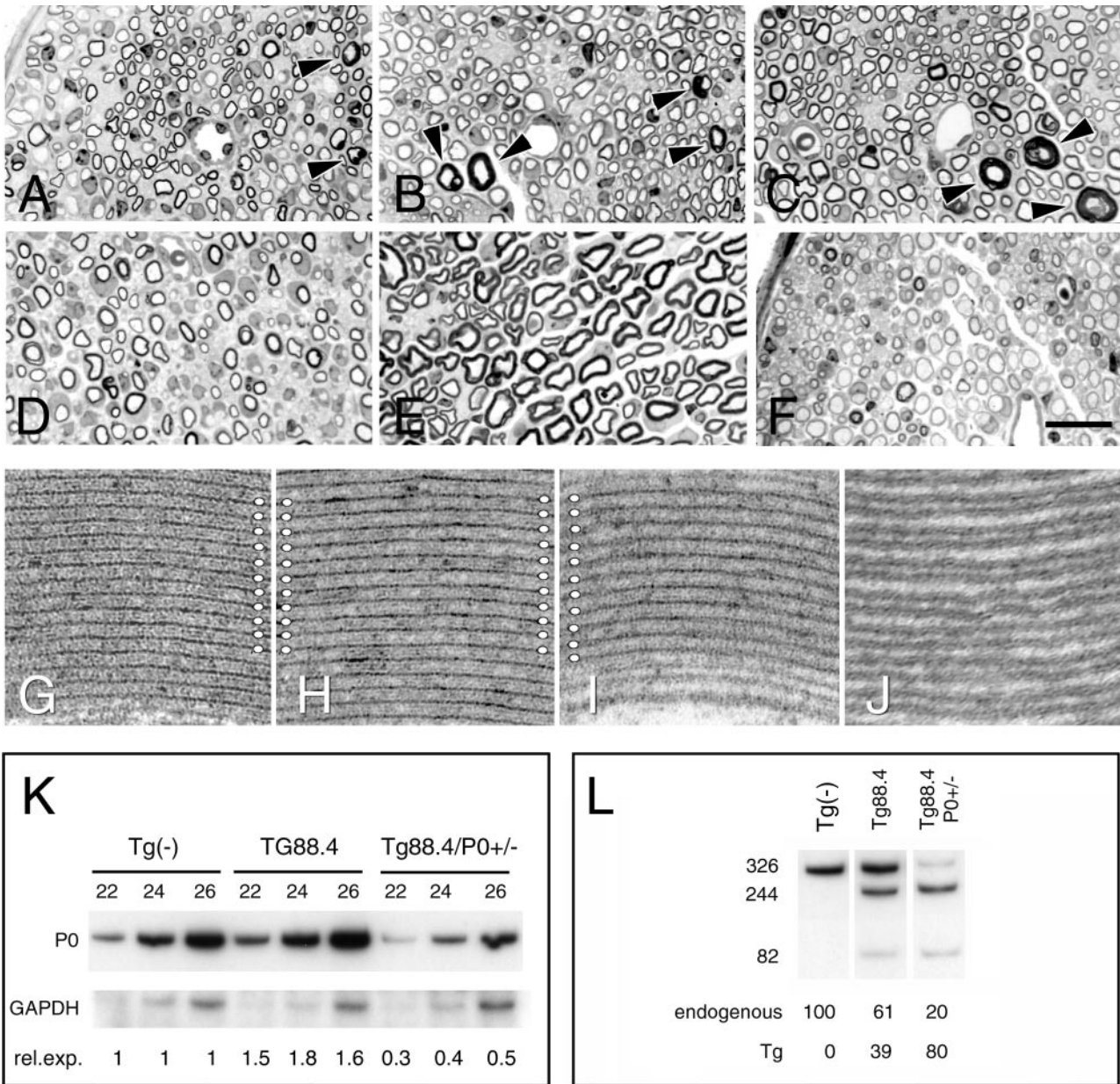
Figure 7. Myelin uncompaction and tomacula are not rescued in the *Mpz* null background. P_0myc/Tg 88.4 was crossed into the *Mpz* heterozygous and homozygous null background, and sciatic nerves from P28 offspring were analyzed. Semithin sections of (A) Tg 88.4 (P_0myc), (B) Tg 88.4/$P_0^{-/-}$, (C) Tg 88.4/$P_0^{+/-}$, (D) Tg 80.4 (P_0wt), (E) Tg 80.4/$P_0^{-/-}$, and (F) $P_0^{-/-}$ show that, whereas lowering the dosage of P_0 rescues dysmyelination in Tg80 (P_0wt overexpressor) mice (compare D to E), it exacerbates tomacula in Tg 88 (P_0myc) mice (B and C, arrows). EM analysis of the myelin sheaths (in each case, the area of the best "compaction" is shown) of (G) nontransgenic, (H) Tg 88.4/$P_0^{+/-}$, (I) Tg 88.4/$P_0^{-/-}$, (J) $P_0^{-/-}$ reveals that when P_0myc is expressed (I) alone it can compact myelin lamellae, however in I the space of 10 periods (11 MDL marked by white circles) is larger than that formed by (G) P_0wt or a mixture of (H) P_0myc and P_0wt. 10 periods = 156 $\pm$ 2.3 nm (mean $\pm$ SEM) in G ($n =$ 9) and 175 $\pm$ 4.6 nm in I ($n = 8$), $P < 0.001$ by Student's *t* test, which is equivalent to a 12% increase. Increasing the magnification, such that the double IPLs are visible, shows that this increase is due to a widened space between IPL in I compared with G (data not shown). Note that in contrast to what was reported previously in $P_0^{-/-}$ mice on an inbred mixed 129Sv/C57BL/6J background (Giese et al., 1992), in (J) $P_0^{-/-}$ FVB congenic mice, most fibers do not form either IPL or MDL. (K) Semiquantitative RT-PCR analysis from P28 sciatic nerves shows that total levels of P_0 mRNA are reduced in Tg 88.4/$P_0^{+/-}$ compared with nontransgenic or P_0myc/Tg 88.4 nerves. Relative expression (rel. exp) is the quotient of the densitometric values of P_0 divided by GAPDH; the quotient obtained in the nontransgenic (Tg$^-$) is arbitrarily defined as one. (L) Digestion with DpnII allows endogenous (326-nt band) and transgenic (244- and 82-nt bands) P_0 signals to be distinguished. The level of endogenous P_0 is decreased out of proportion in Tg 88.4/$P_0^{+/-}$ (predicted ratio of P_0myc/$P_0 \sim$50:50, not 80:20), suggesting that P_0myc has a dominant-negative effect on the expression of endogenous *Mpz*. Bar: (A–F) 50 μm; (G–J) 60 nm.

present in enlarged fibers (Fig. 6 B). The majority of fibers expressed P_0myc. A few fibers, apparently normal in caliber, expressed only wt P_0 (Fig. 6 A, asterisk).

To determine if P_0myc protein was present in the uncompacted myelin lamellae, we performed double immunoelectron microscopy for P_0 and P_0myc. Fig. 6 C shows that both P_0 (small gold particles) and P_0myc (large gold particles) are present in the widened myelin lamellae. Both P_0 and P_0myc were found in normal myelin, as well. Thus, the transgenic protein is incorporated into the ma-
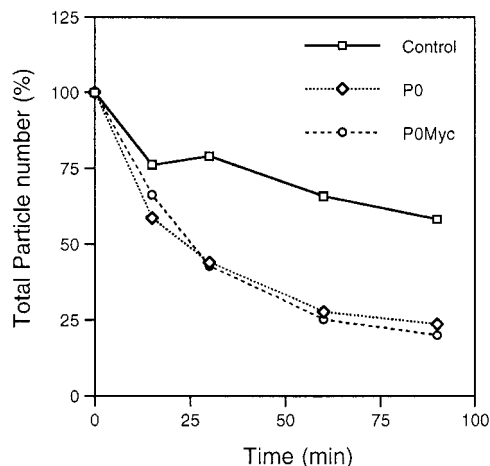
Figure 8. Aggregation properties of P_0myc-expressing cells. Single cell suspensions of CHO cells expressing P_0wt, P_0myc, and control transfected cells were allowed to aggregate. Samples were withdrawn at intervals and the total particle number was counted in a light microscope. The mean percent of initial total particle number $\pm$ SEM ($n = 3$) was plotted against time. Cells transfected with P_0myc aggregated identically to those transfected with P_0wt.

jority of myelin sheaths, and it is present both in tomacula and widened myelin lamellae. Furthermore, though anti-P_0 antibodies recognize epitopes on both P_0 and P_0myc, P_0myc is not likely to account for all of the P_0 staining detected, as Western blot analysis revealed similar amounts of P_0 and P_0myc in nerves of this line (P_0myc/88.4), and immunohistochemical analysis showed that only rare fibers contained P_0 alone. Thus, it is very likely that P_0 and P_0myc are cointegrated in most myelin sheaths.

The Phenotype of P_0myc Mice Is Not Rescued by Decreasing or Removing wt P_0

To analyze the effect of P_0myc in the absence of P_0wt, we crossed the P_0myc/88.4 line into the P_0 null background and analyzed sciatic nerves at P28. A similar experiment performed in a line of mice that overexpressed comparable levels of wt P_0 (Tg80.4; Wrabetz et al., 2000) completely rescued the hypomyelination due to P_0 overexpression (compare Fig. 7, D and E). In contrast, hypomyelination is only slightly improved for P_0myc in either the $P_0^{+/-}$ or $P_0^{-/-}$ backgrounds (compare Fig. 7, B and C to A). More strikingly, tomacula and abnormal compaction (see below) were not improved by lowering the dosage of P_0, rather they worsened. Tomacula were rarely seen at P28 in cross sections of P_0myc/$P_0^{+/+}$ mice, but were readily observed in cross-sections of P_0myc/$P_0^{+/-}$ and P_0myc/$P_0^{-/-}$ mice (Fig. 7, B and C, arrowheads). Nerve conduction velocities also remained low in two P_0myc lines in the $P_0^{+/-}$ background (88.4 and 88.1; Fig. 2). These data strongly suggest that abnormal compaction of myelin, tomacula, and low nerve conduction velocities are due to the presence of P_0myc.

The kind of compaction abnormalities seen in these experiments provided insight into the mechanism by which P_0myc causes dysmyelination. The proportion of myelinated fibers with abnormally compacted myelin was ~11% in P_0myc/$P_0^{+/+}$, 35% in P_0myc/$P_0^{+/-}$, and 100% in P_0myc/$P_0^{-/-}$ mice. We observed two types of abnormally

compacted fibers in P_0myc/$P_0^{-/-}$: (a) rare fibers in which both the intraperiod and MDL were absent (data not shown) and (b) majority of fibers with myelin that appeared compacted, but had abnormal periodicity due to a wide (but not absent) IPL (Fig. 7, compare I to G). In contrast, most fibers of $P_0^{-/-}$ mice in the FVB congenic background formed neither an IPL, nor a MDL (Fig. 7 J). These data suggest that P_0myc molecules are partially adhesive, since they can interact homotypically to form an IPL, but they are not able to compact it tightly.

We noticed that in the P_0myc/$P_0^{+/-}$ and P_0myc/$P_0^{-/-}$ mice the myelin sheaths were thinner than normal. Such hypomyelination could reflect either mild overexpression or reduced expression of P_0, since in the FVB/N background, $P_0^{+/-}$ showed slight hypomyelination at P28 (Wrabetz et al., 2000). To distinguish between these two possibilities, we compared total P_0 mRNA levels in nontransgenic, P_0myc, and P_0myc/$P_0^{+/-}$ sciatic nerves by semiquantitative RT-PCR. Fig. 7 K shows that the total levels of P_0 mRNA were reduced more than expected in P_0myc/$P_0^{+/-}$ sciatic nerves compared with nontransgenic and P_0myc nerves (expected relative expression should be roughly one). This indicates that the hypomyelination in P_0myc/$P_0^{+/-}$ mice is likely due to underexpression of P_0. To understand why the total level of P_0 mRNA in P_0myc/$P_0^{+/-}$ was reduced, we digested the RT-PCR product with DpnII to distinguish the contribution of transgenic P_0 versus wt P_0 to the observed levels. Fig. 7 L shows that the levels of endogenous P_0 are decreased out of proportion in P_0myc/$P_0^{+/-}$ nerves, suggesting that P_0myc interferes not only with P_0 adhesion, but also with the expression of endogenous P_0.

P_0myc Protein Is Adhesive in an Aggregation Assay In Vitro

Despite the severe phenotype of P_0myc mice, myelin is more compacted in P_0myc/$P_0^{-/-}$ mice than in $P_0^{-/-}$ mice, suggesting that the P_0myc protein is at least partially adhesive. To measure the adhesiveness of P_0myc, we expressed the P_0myc protein in CHO cells and measured its homotypic adhesion and compared it with wt P_0. Fig. 8 shows that P_0wt and P_0myc are equally adhesive in this assay. To ask if P_0myc could adhere to P_0wt, we mixed P_0wt- and P_0myc-expressing cells and examined the composition of aggregates. The aggregates had an equal distribution of P_0myc and P_0wt cells (data not shown; Filbin, M.T., manuscript in preparation). Therefore, P_0myc retains the ability to mediate homotypic interaction, and it adhered with the same affinity to itself and to P_0wt.

Discussion

Here, we describe the behavioral, electrophysiological, and morphological alterations of transgenic mice carrying an epitope (myc) tag at the NH$_2$ terminus of the P_0 glycoprotein, along with normal P_0. Surprisingly, P_0myc mice manifested peripheral nerve abnormalities typical of two subtypes of CMT1B, including tomacula and disruption of IPLs. This phenotype differed from that of P_0 overexpression and was not rescued in P_0myc/P_0 null mice. P_0myc acted via gain of function, as it was incorporated into myelin and present in morphological abnormalities. In addi-

tion, P_0myc was adhesive, as it aggregated transfected cells equally to wt P_0. These data underline that P_0 structural interactions in myelin are complex and provide insights into the normal role of P_0 in myelin compaction. P_0myc mice provide the first model of CMT1B due to gain of function and prove that myelin packing abnormalities result from either loss or gain of P_0 function.

Pathological Findings in P0myc Mice Are Due to the Expression of the mP0TOT(myc) Transgene

The pathological features observed in P_0myc mice could be due to the ectopic expression of the transgene or, since the peripheral nerve myelination is highly susceptible to increased *Mpz* dosage (Wrabetz et al., 2000), to overexpression of P_0. The observed phenotype is not due to ectopic expression, since a transgenic vector with the same regulatory sequences of mP_0TOT(myc) was expressed with the same cell and developmental specificity as endogenous P_0 (Feltri et al., 1999), and an identical transgene, but without a myc tag, could produce morphologically normal myelin (Wrabetz et al., 2000).

In addition, tomacula and widened lamellae in P_0myc mice are not due to increased *Mpz* dosage. First, they persist independently from the total levels of P_0. Second, they are observed in the absence of pathological P_0 overexpression: dysmyelination appears at ~0.5-fold overexpression (Wrabetz et al., 2000) and the P_0myc/88.4 line showed mild overexpression (0.4-fold), which is compatible with normal PNS myelination. A further reduction of total P_0 by breeding P_0myc/88.4 into $P_0^{+/-}$ or $P_0^{-/-}$ backgrounds did not rescue myelin uncompaction and tomacula or altered conduction velocities. Finally, neither myelin uncompaction nor tomacula were ever observed in multiple lines of transgenic mice overexpressing P_0wt over a wide range.

P0myc Is Partially Adhesive

In vitro assay showed that P_0myc and P_0 are equally adhesive. However, when P_0myc was the only P_0 present in the myelin sheath (P_0myc/$P_0^{-/-}$ mice), it only partially compacted myelin lamellae. One interpretation of these results is that P_0myc is partially adhesive due to gain of abnormal function. P_0 emanates from the membrane as a tetramer and each tetramer interacts in trans with four surrounding tetramers protruding from the opposite membrane (Shapiro et al., 1996). These interactions involve several ectodomains, in particular the BC loop (Shapiro et al., 1996) and residue tryptophan 28, which is thought to interact directly with the apposing lipid bilayer (Shapiro et al., 1996). The combination of these interactions are thought to determine the spacing of the IPLs (Shapiro et al., 1996). In this model, the NH_2 terminus is apposed to the BC loop such that the myc tag attached to the NH_2 terminus could impair interactions between this region and opposing tetramers, as well as tryptophan 28 with the lipid bilayer (Shapiro et al., 1996), leading to widening of the IPL. In agreement with this, we show that IPLs formed by myc in P_0myc/$P_0^{-/-}$ mice are larger than those formed by P_0wt. Although partially defective, P_0myc could still permit initial adhesion between membranes in the cell assay, yet interfere with tight compaction as it normally occurs in myelin. Although the space between extracellular leaflets in apposing myelin lamellae varies with fixation (King and

Thomas, 1984; Kirschner et al., 1996a), the space between membranes in adherent P_0-transfected cell lines is probably consistently larger than the space found in compact myelin (D'Urso et al., 1990; Filbin et al., 1990; Spiryda, 1998; Yin et al., 2000).

The putative impaired adhesiveness of P_0myc may actually protect against P_0 overexpression. High overexpression of P_0 causes dysmyelination due to abnormal appearance of P_0 in the spiraling mesaxons, resulting in obligate homotypic interactions and arrested myelination (Yin et al., 2000). In contrast, this was never observed in line P_0myc/88.2, despite similar levels of transgenic P_0 overexpression. This also supports that P_0myc is less adhesive than P_0wt.

"Dominant-Negative" Is the Predominant Pathogenetic Mechanism: Implication for the Formation of IPL and a Normal Role of P0 in Myelin Compaction

Our data allow us to speculate whether P_0myc acts through a mechanism of loss or gain of function, and, within gain of function, whether it is dominant-negative or toxic. These distinctions are important, since different mechanisms might imply different therapeutic approaches for P_0 ECD mutations in CMT1B patients.

Loss of function of P_0myc cannot be the pathogenetic mechanism, since P_0myc mice contain two normal *Mpz* alleles. Furthermore, RT-PCR and Western blot analysis showed normal amounts of P_0wt mRNA and protein in P_0myc mice. For the mP_0TOT(myc) transgene to act via gain of function, it must be expressed. Immunolocalization demonstrated that P_0myc was expressed in myelinating SCs, inserted in the myelin sheaths, and associated with widened myelin lamellae and tomacula. Although anti-P_0 antibodies recognize both P_0wt and P_0myc, it is reasonable to assume that P_0 and P_0myc colocalize. In fact, Western blot analysis, in which wt and mutated protein are distinguishable by size, showed a comparable amount of wt and P_0myc protein in lines 88.4 and 88.1 (Fig. 5). Since P_0myc is detected in most myelin sheaths (one rare exception is the green fiber shown in Fig. 7 B), the expression of P_0wt in these cells is presumably comparable. Thus, mP_0TOT(myc) acts through gain of function at the cellular level.

Our data suggests that P_0myc does not act through a toxic mechanism. If toxicity was the primary mechanism at work, the effect of P_0myc should increase in parallel with its dosage and should be independent of the amount of P_0wt. Instead, we observe the opposite, suggesting that P_0myc behaves as a dominant-negative. Since P_0myc and P_0wt colocalize in myelin, and an in vitro assay shows that they can adhere to each other, P_0myc probably have a dominant-negative effect both on P_0wt and itself.

Finally, we provide evidence that P_0myc also decreases P_0wt mRNA levels. By outcrossing P_0myc/88.4 line into the $P_0^{+/-}$ background we expected to decrease the amount of wt P_0 message by one half, but we observed that it fell instead to one eighth. This suggests that P_0myc may directly exert a negative effect on the expression of *Mpz*. The mechanism underlying this finding is presently unknown.

P0myc As a Model of Subtypes of CMT1B

The phenotype of P_0myc mice is characterized by distal atrophy, tremor, low nerve conduction velocity, and dysmyelination with widening of myelin lamellae and tomacula.

Similar pathological findings are described in two subgroups of patients affected by CMT1B due to mutations in the ECD of P_0. Nerve biopsies of these patients usually manifest either myelin uncompaction or tomacula (Gabreels-Festen et al., 1996). Abnormalities of myelin compaction are found in substitution Arg69Cys, Arg69His, Thr5Ile, and ΔSer34 (Gabreels-Festen et al., 1996; Kirschner et al., 1996b; Ohnishi et al., 1999). Usually in these patients, both IPL and MDL are absent, but in some cases the IPL is predominantly affected (Arg69His and Arg69Cys) (Kirschner et al., 1996b; Ohnishi et al., 1999). Instead, other mutations, including Ile33Phe, Ser49Leu, Lys67Glu, Asn93Ser, Lys101Arg, Asn102Lys, and Ile106Leu, result in demyelinating neuropathy associated with focally abnormal folded myelin or tomacula (Thomas et al., 1994; Gabreels-Festen et al., 1996; Nagakawa et al., 1999; Planté-Bordeneuve et al., 1999; Sindou et al., 1999).

Of note, three of the point mutations in P_0 ECD causing tomacula involve residues (101, 102, and 106) present in the FG loop, which also resides in proximity of the NH_2 terminus (Shapiro et al., 1996). The FG loop does not appear to be involved in P_0 homotypic interaction (Shapiro et al., 1996) and, therefore, could be free to perform a different function (e.g., putative interaction with PMP-22, see below), that, if perturbed, leads to tomacula formation. Interestingly, as mentioned before, point mutations in CMT1B usually result in either myelin packing abnormalities or tomacula, but usually not both (Gabreels-Festen et al., 1996). Thus, 13 amino acids of myc at the NH_2 terminus of P_0 could disrupt interactions of multiple domains of P_0 situated nearby (e.g., the BC and FG loops), resulting in both packing abnormalities and tomacula.

Tomacula formation or abnormal myelin focal folding is rare in CMT1B, whereas it is more common in CMT1A and HNPP (Windebank, 1993). In mice, a tomaculous neuropathy is observed after inactivation of *Pmp-22*, myelin-associated glycoprotein (*Mag*), or periaxin genes (Adlkofer et al., 1997; Carenini et al., 1997; Yin et al., 1998; Gillespie et al., 2000), and, in this report, in mutation of *Mpz*. Since deletion or overexpression of P_0 does not result in tomacula formation, it is more likely that an acquired function of P_0myc could cause hypermyelination. Recently, evidence for physical interactions between P_0 and PMP-22 has been proposed (D'Urso et al., 1999), suggesting that P_0myc may have a trans-dominant–negative effect on PMP-22.

In this light, it is interesting to note that Roussy-Levy syndrome, often due to PMP-22 duplication (Thomas et al., 1997), can also be due to a mutation in the ECD of P_0 (Asn102Lys). Nerve biopsies from these patients reveal focally folded myelin sheaths and often absence of onion bulbs (Planté-Bordeneuve et al., 1999). Roussy-Levy patients were originally considered distinct from CMT because of a particular combination of clinical symptoms including tremor, ataxia, and distal atrophy. Since P_0myc mice present with tremor, distal atrophy, probable sensory symptoms (self-induced skin lesions), focally folded myelin, and no onion bulbs, they could be considered a model of Roussy-Levy syndrome.

In summary, our data suggest that P_0myc mice could provide insights into the pathogenesis and treatment of a subgroup of CMT patients. Interestingly, our data already suggest a potential therapeutic approach. Crossing of P_0myc mice into the P_0 null background shows that the phenotype is worsened as the relative amount of P_0wt is lowered. Hence, increasing the dosage of P_0wt could counteract the effect of the mutated P_0, as long as the threshold of overexpression that causes dysmyelination is not exceeded. This threshold is relatively low during development (Wrabetz et al., 2000), but reflects the effects of abnormal expression of P_0 in an early phase of myelinogenesis (Yin et al., 2000). Instead, the threshold for abnormalities may be higher when P_0 overexpression begins in adulthood.

References

Adlkofer, K., R. Frei, K.-H. Neuberg, J. Zielasek, K. Toyka, and U. Suter. 1997. Heterozygous peripheral myelin protein 22-deficient mice are affected by a progressive demyelinating tomaculous neuropathy. *J. Neurosci.* 17:4662–4671.

Archelos, J.J., K. Roggenbuck, J. Schneider-Schaulies, C. Linington, K.V. Toyka, and H.P. Hartung. 1993. Production and characterization of monoclonal antibodies to the extracellular domain of P0. *J. Neurosci. Res.* 35:46–53.

Brinster, R.L., H.Y. Chen, M.E. Trumbauer, M.K. Yagle, and R.D. Palmiter. 1985. Factors affecting the efficiency of introducing foreign DNA into mice by microinjecting eggs. *Proc. Natl. Acad. Sci. USA.* 82:4438–4442.

Carenini, S., D. Montag, H. Cremer, M. Schachner, and R. Martini. 1997. Absence of the myelin-associated glycoprotein (MAG) and the neural cell adhesion molecule (NCAM) interferes with the maintenance, but not the formation of peripheral myelin. *Cell Tissue Res.* 287:3–9.

Colman, D., G. Kreibich, A. Frey, and D. Sabatini. 1982. Synthesis and incorporation of myelin polypeptides into CNS myelin. *J. Cell Biol.* 95:598–608.

D'Urso, D., P.J. Brophy, S.M. Staugaitis, C.S. Gillespie, A.B. Frey, J.G. Stempak, and D.R. Colman. 1990. Protein zero of peripheral nerve myelin: biosynthesis, membrane insertion, and evidence for homotypic interaction. *Neuron.* 4:449–460.

D'Urso, D., P. Ehrhardt, and H. Mueller. 1999. Peripheral myelin protein 22 and protein zero: a novel association in peripheral nervous system myelin. *J. Neurosci.* 19:3395–3403.

Feltri, M., M. D'Antonio, A. Quattrini, R. Numerato, M. Arona, S. Previtali, S.-Y. Chiu, A. Messing, and L. Wrabetz. 1999. A novel P0 glycoprotein transgene activates expression of lacZ in myelin-forming Schwann cells. *Eur. J. Neurosci.* 11:1577–1586.

Fiering, S., E. Epner, K. Robinson, Y. Zhuang, A. Telling, M. Hu, D.I. Martin, T. Enver, T.J. Ley, and M. Groudine. 1995. Targeted deletion of 5′HS2 of the murine beta-globin LCR reveals that it is not essential for proper regulation of the beta-globin locus. *Genes Dev.* 9:2203–2213.

Filbin, M., and G. Tennekoon. 1990. High level of expression of the myelin protein P0 in Chinese hamster ovary cells. *J. Neurochem.* 55:500–505.

Filbin, M., and G. Tennekoon. 1993. Both P0-molecules must be glycosylated for homophilic adhesion. *J. Cell Biol.* 122:451–459.

Filbin, M., F. Walsh, B. Trapp, J. Pizzey, and G. Tennekoon. 1990. Role of myelin Po protein as a homophilic adhesion molecule. *Nature.* 344:871–872.

Gabreels-Festen, A., J. Hoogendijk, P. Meijerink, F. Gabreels, P. Bolhuis, S. van Beersum, T. Kulkens, E. Nelis, F. Jennekens, M. de Visser, B. van Engelen, C. van Broeckhoven, and E. Mariman. 1996. Two divergent types of nerve pathology in patients with different Po mutations in Charcot-Marie-Tooth disease. *Neurology.* 47:761–765.

Giese, K.P., R. Martini, G. Lemke, P. Soriano, and M. Schachner. 1992. Mouse P0 gene disruption leads to hypomyelination, abnormal expression of recognition molecules, and degeneration of myelin and axons. *Cell.* 71:565–576.

Gillespie, C.S., D.L. Sherman, S.M. Fleetwood-Walker, D.F. Cottrell, S. Tait, E.M. Garry, V.C. Wallace, J. Ure, I.R. Griffiths, A. Smith, and P.J. Brophy. 2000. Peripheral demyelination and neuropathic pain behavior in periaxin-deficient mice. *Neuron.* 26:523–531.

Harding, A.E. 1995. From the syndrome of Charcot, Marie and Tooth to disor-

ders of peripheral myelin proteins. *Brain.* 118:809–818.

King, R.H., and P.K. Thomas. 1984. The occurrence and significance of myelin with unusually large periodicity. *Acta Neuropathol.* 63:319–329.

Kirschner, D.A., H. Inouye, and R.A. Saavedra. 1996a. Membrane adhesion in peripheral myelin: good and bad wraps with protein Po. *Structure.* 4:1239–1244.

Kirschner, D.A., K. Szumowski, A. Gabreel-Festen, J.E. Hoogendijk, and P.A. Bolhuis. 1996b. Inherited demyelinating peripheral neuropathies: relating myelin packing abnormalities to Po molecular defects. *J. Neurosci. Res.* 46:502–508.

Lemke, G., E. Lamar, J. Patterson. 1988. Isolation and analysis of the gene encoding peripheral myelin protein zero. *Neuron.* 1:73–83.

Martini, R. 1997. Animal models for inherited peripheral neuropathies. *J. Anat.* 191:321–336.

Martini, R., J. Zielasek, K.V. Toyka, K.P. Giese, and M. Schachner. 1995. Protein zero (P0)-deficient mice show myelin degeneration in peripheral nerves characteristic of inherited human neuropathies. *Nat. Genet.* 11:281–286.

Nagakawa, M., M. Suehara, A. Saito, H. Takashima, F. Umehara, M. Saito, N. Kanzato, T. Matsuzaki, S. Takenaga, S. Sakoda, S. Izumo, and M. Osame. 1999. A novel MPZ gene mutation in dominantly inherited neuropathy with focally folded myelin sheaths. *Neurology.* 52:1271–1275.

Nelis, E., N. Haites, and C. Van Broeckhoven. 1999. Mutations in the peripheral myelin genes and associated genes in inherited peripheral neuropathies. *Hum. Mutat.* 13:11–28.

Ohnishi, A., T. Yamamoto, S. Yamamori, K. Sudo, Y. Fukushima, and M. Ikeda. 1999. Myelinated fibers in Charcot-Marie-Tooth disease type 1B with Arg98His mutation of Po protein. *J. Neurol. Sci.* 171:97–109.

Planté-Bordeneuve, V., A. Guiochon-Mantel, C. Lacroix, J. Lapresle, and G. Said. 1999. The Roussy-Lévy family: from the original description to the gene. *Ann. Neurol.* 46:770–773.

Quattrini, A., S. Previtali, M.L. Feltri, N. Canal, R. Nemni, and L. Wrabetz. 1996. β4 integrin and other Schwann cell markers in axonal neuropathy. *Glia.* 17:294–306.

Schneider-Schaulies, J., A.V. Brunn, and M. Schachner. 1990. Recombinant peripheral myelin protein Po confers both adhesion and neurite outgrowth–promoting properties. *J. Neurosci. Res.* 27:286–297.

Shapiro, L., J.P. Doyle, P. Hensley, D. Colman, and W.A. Hendrickson. 1996. Crystal structure of the extracellular domain from Po, the major structural protein of peripheral nerve myelin. *Neuron.* 17:435–449.

Sindou, P., J.-M. Vallat, F. Chapon, J. Archelos, F. Tabaraud, T. Anani, K. Braund, T. Maisonobe, J.-J. Hauw, and A. Vandenberghe. 1999. Ultrastructural protein zero expression in Charcot-Marie-Tooth type 1B disease. *Muscle Nerve.* 22:99–104.

Spiryda, L. 1998. Myelin protein zero and membrane adhesion. *J. Neurosci. Res.* 54:137–146.

Tachi, N., N. Kozuka, K. Ohya, S. Chiba, and K. Sasaki. 1997. Tomaculous neuropathy in Charcot-Marie-Tooth disease with myelin protein zero gene mutation. *J. Neurol. Sci.* 153:106–109.

Thomas, F.P., R.V. Lebo, G. Rosoklija, X.S. Ding, R.E. Lovelace, N. Latov, and A.P. Hays. 1994. Tomaculous neuropathy in chromosome 1 Charcot-Marie-Tooth syndrome. *Acta Neuropathol. (Berl.).* 87:91–97.

Thomas, P.K., W. Marques, Jr., M.B. Davis, M.G. Sweeney, R.H. King, J.L. Bradley, J.R. Muddle, J. Tyson, S. Malcolm, and A.E. Harding. 1997. The phenotypic manifestations of chromosome 17p11.2 duplication. *Brain.* 120:465–478.

Villa, A., P. Podini, M. Panzeri, H. Soling, P. Volpe, and J. Meldolesi. 1993. The endoplasmic-sarcoplasmic reticulum of smooth muscle: immunocytochemistry of vas deferens fibers reveals specialized subcompartments differently equipped for the control of Ca^{2+} homeostasis. *J. Cell Biol.* 121:1041–1051.

Warner, L.E., M.J. Hilz, S.T. Appel, J.M. Killian, E.H. Kolodny, G. Karpati, S. Carpenter, G.V. Watters, C. Wheeler, D. Witt, A. Bodell, E. Nelis, C.V. Broeckhoven, and J.R. Lupski. 1996. Clinical phenotypes of different MPZ (Po) mutations may include Charcot-Marie-Tooth type 1b, Dejerine-Sottas, and congenital hypomyelination. *Neuron.* 17:451–460.

Windebank, A. 1993. Inherited recurrent focal neuropathies. *In* Peripheral Neuropathy. P. Dyck, P. Thomas, J. Griffin, P. Low, and I. Poduslo, editors. W.B. Saunders Co., Philadelphia. 1137–1148.

Wong, M.H., and M.T. Filbin. 1996. Dominant-negative effect on adhesion by myelin Po protein truncated in its cytoplasmic domain. *J. Cell Biol.* 134:1531–1541.

Wrabetz, L., M. Feltri, C. Hanemann, and H. Müller. 2001. The molecular genetics of hereditary demyelinating neuropathies. *In* Glial Cell Development: Basic Principles and Clinical Relevance. K. Jessen and W. Richardson, editors. Oxford University Press, Oxford. In press.

Wrabetz, L., M.L. Feltri, A. Quattrini, D. Imperiale, S. Previtali, M. D'Antonio, R. Martini, X. Yin, B.D. Trapp, L. Zhou, S.-Y. Chiu, and A. Messing. 2000. P_0 overexpression causes congenital hypomyelination of peripheral nerves. *J. Cell Biol.* 148:1021–1033.

Yin, X., T. Crawford, J. Griffin, P.-h. Tu, V.-Y. Lee, C. Li, J. Roder, and B. Trapp. 1998. Myelin-associated glycoprotein is a myelin signal that modulates the caliber of myelinated axons. *J. Neurosci.* 18:1953–1962.

Yin, X., G.J. Kidd, L. Wrabetz, M.L. Feltri, A. Messing, and B.D. Trapp. 2000. Schwann cell myelination requires timely and precise targeting of P_0 protein. *J. Cell Biol.* 148:1009–1020.